Dispensability of Glutamic Acid 48 and Aspartic Acid 134 for Mn^{2+}-Dependent Activity of *Escherichia coli* Ribonuclease HI†

Yasuo Tsunaka,‡ Mitsuru Haruki,‡,§ Masaaki Morikawa,‡ Motohisa Oobatake,|| and Shigenori Kanaya*,‡

Department of Material and Life Science, Graduate School of Engineering, Osaka University, 2-1 Yamadaoka, Suita, Osaka 565-0871, Japan, and Faculty of Science and Technology, Meijo University, 1-501, Shiogamaguchi, Tenpaku-ku, Nagoya 468-8502, Japan

Received August 28, 2002; Revised Manuscript Received January 31, 2003

ABSTRACT: The activities of the eight mutant proteins of *Escherichia coli* RNase HI, in which the four carboxylic amino acids (Asp^{10}, Glu^{48}, Asp^{70}, and Asp^{134}) involved in catalysis are changed to Asn (Gln) or Ala, were examined in the presence of Mn^{2+}. Of these proteins, the E48A, E48Q, D134A, and D134N proteins exhibited the activity, indicating that Glu^{48} and Asp^{134} are dispensable for Mn^{2+}-dependent activity. The maximal activities of the E48A and D134A proteins were comparable to that of the wild-type protein. However, unlike the wild-type protein, these mutant proteins exhibited the maximal activities in the presence of >100 μM $MnCl_2$, and their activities were not inhibited at higher Mn^{2+} concentrations (up to 10 mM). The wild-type protein contains two Mn^{2+} binding sites and is activated upon binding of one Mn^{2+} ion at site 1 at low (~1 μM) Mn^{2+} concentrations. This activity is attenuated upon binding of a second Mn^{2+} ion at site 2 at high (>10 μM) Mn^{2+} concentrations. The cleavage specificities of the mutant proteins, which were examined using oligomeric substrates at high Mn^{2+} concentrations, were identical to that of the wild-type protein at low Mn^{2+} concentrations but were different from that of the wild-type protein at high Mn^{2+} concentrations. These results suggest that one Mn^{2+} ion binds to the E48A, E48Q, D134A, and D134N proteins at site 1 or a nearby site with weaker affinities. The binding analyses of the Mn^{2+} ion to these proteins in the absence of the substrate support this hypothesis. When Mn^{2+} ion is used as a metal cofactor, the Mn^{2+} ion itself, instead of Glu^{48} and Asp^{134}, probably holds water molecules required for activity.

Ribonuclease H (RNase H) hydrolyzes only the RNA strand of the RNA/DNA hybrid (*1*). The enzyme is ubiquitously present in various organisms. On the basis of the difference in the amino acid sequences, they are classified into two major families, type 1 and type 2 RNases H (*2*, *3*). Bacterial RNase HI,[1] eukaryotic RNase H1, and the RNase H domain of retroviral reverse transcriptase (RT) are the members of type 1 RNases H. Bacterial RNases HII and HIII, archaeal RNase HII, and eukaryotic RNase H2 are the members of type 2 RNases H. A single archaeal genome contains a single gene encoding RNase H (RNase HII), whereas single bacterial and eukaryotic genomes often contain multiple genes encoding different RNases H (*3*). A *Bacillus subtilis* mutant lacking all functional RNases H (RNases HII and HIII) exhibits a lethal growth phenotype (*4*). An *Escherichia coli* mutant lacking all functional RNases H (RNases HI and HII) exhibits a temperature-sensitive growth phenotype (*4*). A *Saccharomyces cerevisiae* mutant lacking all functional RNases H (RNases H1 and H2) exhibits altered sensitivities to hydroxyurea, ethyl methanesulfonate, and caffeine (*5*). These results suggest that RNases H are involved in important cellular processes. In fact, RNases H have been suggested to be involved in DNA replication, repair, and/or transcription (*6*−*9*). However, their physiological roles remain to be fully understood. In contrast, the retroviral RNase H activity has been shown to be required to convert genomic RNA to double-stranded DNA and is, therefore, indispensable for proliferation of retroviruses (*10*).

Comparison of the crystal structures of *E. coli* RNase HI (*11*, *12*) and *Thermococcus kodakaraensis* RNase HII (*13*), which are members of type 1 and type 2 RNases H, respectively, revealed that these two enzymes share a main chain fold consisting of a five-stranded β-sheet and two α-helices. In addition, steric configurations of the four acidic active site residues are conserved in these two structures. These results suggest that type 1 and type 2 RNases H hydrolyze substrates through a similar mechanism. In addition to these RNases H, various functionally unrelated enzymes, such as resolvase (*14*), integrase (*15*, *16*), transposase (*17*), exonuclease III (*18*), and ribonuclease III (*19*), recognize double-stranded nucleic acids and hydrolyze phosphodiester bonds to generate 5′-phosphate and 3′-hydroxy termini. A characteristic common to these enzymes, which are members of the polynucleotidyl transferase superfamily, is a high negative-charge density at the active site,

† Dedicated to the memory of the late Dr. Motohisa Oobatake.

* To whom correspondence should be addressed. Tel/Fax: +81-6-6879-7938. E-mail: kanaya@mls.eng.osaka-u.ac.jp.

‡ Osaka University.

§ Present address: Department of Materials Chemistry and Engineering, College of Engineering, Nihon University, Tamura-machi, Koriyama, Fukushima 963-8642, Japan.

|| Meijo University.

[1] Abbreviations: RNase HI, ribonuclease HI; RT, reverse transcriptase; CD, circular dichroism.

10.1021/bi0205606 CCC: $25.00
Published on Web 02/28/2003

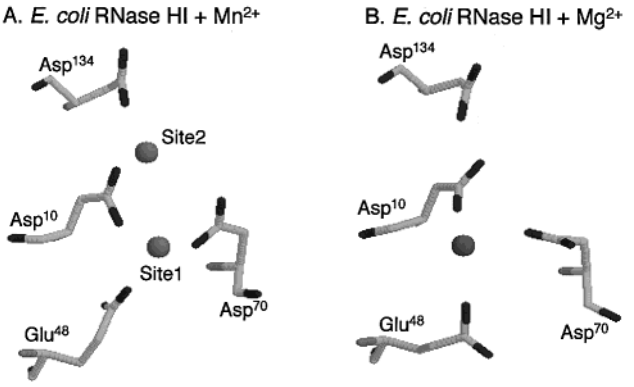

FIGURE 1: Comparison of metal ion coordination in *E. coli* RNase HI. (A) The *E. coli* RNase HI variant with the $Lys^{87} \rightarrow$ Ala mutation was crystallized in the presence of 1 mM $MnCl_2$ (*24*) (Protein Data Bank code 1G15). (B) *E. coli* RNase HI was crystallized in the presence of >100 mM $MgCl_2$ (*23*) (Protein Data Bank code 1RDD). These structures are drawn with the program RasMol.

to which divalent metal ion(s) bind. Therefore, understanding of the catalytic mechanism of one RNase H, regardless of whether it is a type 1 or type 2 enzyme, would offer insight on the catalytic mechanism of the entire superfamily. In this study, we used *E. coli* RNase HI as a model system for investigating the catalytic mechanism of RNase H because the enzyme has been the most extensively studied for structures and functions among the proteins of the RNase H family (*6*, *20*).

E. coli RNase HI is composed of 155 amino acid residues (*21*) and requires Mg^{2+} and Mn^{2+} for activity (*22*). Determination of the crystal structure of the enzyme in complex with Mg^{2+} (*23*) or Mn^{2+} (*24*) indicates that the enzyme contains either a single Mg^{2+}-binding site or two Mn^{2+}-binding sites (sites 1 and 2) (Figure 1). Metal titration experiments using NMR (*25*), CD (*26*), and direct calorimetry (*27*) also suggest that a single Mg^{2+} ion binds to the enzyme. Of the two Mn^{2+}-binding sites, site 1, which is similar to the Mg^{2+}-binding site, is formed by Asp^{10}, Glu^{48}, and Asp^{70}, and site 2 is formed by Asp^{10} and Asp^{134}. These sites are equivalent to those detected in the cocrystal of the RNase H domain of HIV-1 RT with Mn^{2+} (*28*).

The Mn^{2+}- and Mg^{2+}-dependent activities of *E. coli* RNase HI differ with respect to the dependence of enzyme activity on the respective metal ion concentrations (*24*, *29*). The enzyme exhibited the maximal Mn^{2+}- and Mg^{2+}-dependent activities in the presence of 2−5 μM $MnCl_2$ and ∼5 mM $MgCl_2$, respectively. The Mn^{2+}-dependent activity is decreased at higher $MnCl_2$ concentrations. On the basis of these results, an activation/attenuation model has been proposed (*30*). According to this model, binding of one Mn^{2+} or Mg^{2+} ion at site 1 is required for enzyme activation, and binding of a second Mn^{2+} ion at site 2 is inhibitory. A second Mg^{2+} ion does not bind to site 2, probably because the binding affinity of Mg^{2+} is much lower than that of Mn^{2+}.

According to a general acid−base mechanism currently proposed for the catalytic function of *E. coli* RNase HI (*30*), Asp^{10} and Asp^{70} provide ligands for metal binding; His^{124} accepts a proton from the attacking H_2O molecule which acts as a general base; Asp^{134} holds this H_2O molecule; Glu^{48} anchors a second H_2O molecule that acts as a general acid; the metal ion forms an outer sphere complex with the 2′-hydroxyl group of the substrate through an H_2O molecule. These residues have been identified as the active site residues by mutational (*31*−*33*) and structural (*11*, *12*, *34*, *35*) studies. However, the roles of these residues have so far been analyzed almost exclusively for Mg^{2+}-dependent activity.

In this report, we show that Glu^{48} and Asp^{134} are not required for Mn^{2+}-dependent activity of *E. coli* RNase HI. Comparison of the cleavage specificities of the mutant proteins with those of the wild-type proteins in one-metal and two-metal forms, as well as the binding analyses of the Mn^{2+} ion, strongly suggest that one Mn^{2+} ion binds at site 1 or a nearby site of the mutant proteins at Glu^{48} and Asp^{134} with weaker affinities. On the basis of these results, we discuss the catalytic mechanism for Mn^{2+}-dependent activity.

EXPERIMENTAL PROCEDURES

Materials. The wild-type *E. coli* RNase HI protein and its active site mutants (D10N, D10A, E48Q, E48A, D70N, D70A, D134N, and D134A) were previously overproduced and purified (*31*, *33*). In these mutant proteins, Asp^{10} is replaced by Asn (D10N) or Ala (D10A), Glu^{48} is replaced by Gln (E48Q) or Ala (E48A), Asp^{70} is replaced by Asn (D70N) or Ala (D70A), or Asp^{134} is replaced by Asn (D134N) or Ala (D134A). Restriction enzymes and modifying enzymes for recombinant DNA technology were obtained from Takara Shuzo Co., Ltd., [γ-^{32}P]ATP (>5000 Ci/mmol) was from Amersham, and *Crotalus durissus* phosphodiesterase was from Boehringer Mannheim. Other chemicals were of reagent grade.

Cells and Plasmids. Plasmid pJAL600, for the overproduction of the wild-type protein, was previously constructed (*36*). Competent *E. coli* HB101 cells [F^-, *hsd*S20 (r_B^-, m_B^-), *recA13*, *ara-14*, *proA2*, *lacY1*, *galK2*, *rpsL20* (Sm^r), *xyl-5*, *mtl-1*, *supE44*, λ^-] were from Takara Shuzo Co., Ltd.

Mutations. The mutant *rnhA* genes encoding the mutant proteins E48A/D134N and E48A/D134A, in which the codon for Glu^{48} (GAG) is changed to GCG for Ala and the codon for Asp^{134} (GAT) is changed to AAT for Asn or GCT for Ala, were constructed by PCR as described previously (*36*). These mutant *rnhA* genes were substituted for the wild-type *rnhA* gene in plasmid pJAL600, to generate plasmids pJAL48A134N and pJAL48A134A. For overproduction of the mutant proteins E48A/D134N and E48A/D134A, *E. coli* HB101 was transformed with plasmid pJAL48A134N or pJAL48A134A. Overproduction and purification were performed as described previously (*36*).

The protein concentration was determined from the UV absorption, with the assumption that these mutant proteins have the same absorption coefficient, $A_{280}^{0.1\%} = 2.0$, as that of the wild-type protein (*37*). The cellular production level and the purity of these mutant proteins were estimated by 15% SDS−PAGE (*38*), followed by staining with Coomassie Brilliant Blue.

Enzymatic Activity. The RNase H activity was determined at 30 °C for 15 min by measuring the radioactivity of the acid-soluble digestion product from the ^{3}H-labeled M13 DNA/RNA hybrid, as previously described (*39*). The standard assay solution contains 10 mM Tris-HCl (pH 8.0) or 10 mM MES−NaOH (pH 5.5), 50 mM NaCl, 1.4 mM 2-mercaptoethanol (2-ME), 0.05 mg/mL bovine serum albumin (BSA), and the indicated concentrations (0.1 μM−10 mM) of $MnCl_2$ or 10 mM $MgCl_2$. For the analysis of pH

dependence, 10 mM sodium acetate (pH 4.3−5.7), 10 mM MES−NaOH (pH 5.7−7.3), 10 mM Tris-HCl (pH 7.3−9.2), or 10 mM glycine−NaOH (pH 9.2−10.2) was used as the assay buffer. One unit was defined as the amount of enzyme producing 1 μmol of acid-soluble material per 15 min at 30 °C. The specific activity was defined as the enzymatic activity per milligram of protein.

Cleavage of Oligomeric Substrates. The 12 bp RNA/DNA hybrid and 29 bp DNA−RNA−DNA/DNA duplex were prepared by hybridizing 12 b 5′-^{32}P-cggagaugacgg-3′ and 29 b 5′-^{32}P-AATAGAGAAAAAGaaaaAAGATGGCAAAG-3′ with 1.5 molar equiv of the complementary 12 and 29 b DNAs, respectively, as described previously (*2*). In these sequences, RNA and DNA are represented by lower case and upper case letters, respectively. The reaction conditions were the same as that described for the hydrolysis of the M13 DNA/RNA hybrid. The substrate concentration was 1.0 μM. The hydrolysates were separated on a 20% polyacrylamide gel containing 7 M urea and were analyzed with Instant Imager (Packard). The hydrolysates were identified by comparing the migration on the gel with that of oligonucleotides generated by partial digestion of ^{32}P-labeled 12 b RNA or 29 b DNA−RNA−DNA with snake venom phosphodiesterase (*40*).

Circular Dichroism Spectra. The CD spectra were measured on a J-725 spectropolarimeter from Japan Spectroscopic Co., Ltd., at 25 °C in 10 mM sodium acetate (pH 5.5). The protein concentration was 0.13 mg/mL and 0.5−1 mg/mL, and an optical path length of the cell was 2 mm and 10 mm, for the measurement of far-UV and near-UV CD spectra, respectively.

Binding Analysis of Mn^{2+} by Monitoring a Change in Protein Stability. Thermal denaturation curves and the temperature of the midpoint of the transition (T_m) were determined by monitoring the change in the CD value at 220 nm as described previously (*41*). Proteins (0.13 mg/mL) were dissolved in 50 mM glycine−NaOH buffer (pH 9.0) containing 20% glycerin, 2.8 M urea, and various concentrations (0−50 mM) of $MnCl_2$. The free energy change of unfolding (ΔG) at the T_m of the wild-type protein was calculated by the relationship $\Delta G(T) = \Delta H(T) - T\Delta S(T)$, as described previously (*26*).

The dissociation constants of the Mn^{2+} ion were calculated in two ways on the basis of the following assumptions: (1) a single Mn^{2+} ion binds to the protein with the dissociation constant of K_d, and the unfolding equilibrium of the protein in the presence of Mn^{2+} follows a two-state mechanism represented by NL ↔ D + L; (2) two Mn^{2+} ions bind to the protein with the dissociation constants of K_{d1} and K_{d2}, and the unfolding equilibrium of the protein in the presence of Mn^{2+} follows a three-state mechanism represented by NL_2 ↔ NL + L ↔ D + 2L. In these equations, N and D represent the proteins in the native and denatured states, respectively, and L represents the Mn^{2+} concentration. According to Schellman (*42*), the relationship among $\Delta\Delta G$, a_L, and K_d is given by $\Delta\Delta G = \Delta G(L) - \Delta G(L{=}0) = RT \ln(1 + [a_L]/K_d)$, and that among $\Delta\Delta G$, a_L, K_{d1}, and K_{d2} is given by $\Delta\Delta G = \Delta G(L) - \Delta G(L{=}0) = RT \ln(1 + [a_L]/K_{d1} + [a_L^2/K_{d1}K_{d2}])$. $\Delta\Delta G$ represents the difference in the free energy changes of unfolding of the protein in the presence [$\Delta G(L)$] and absence [$\Delta G(L{=}0)$] of Mn^{2+}, at the T_m of the wild-type protein, and a_L represents the activity of the metal ion. The K_d, K_{d1}, and K_{d2} values were calculated from curve fitting of the $\Delta\Delta G$ versus a_L data on the basis of a least-squares analysis.

Binding Analysis of Mn^{2+} by Direct Titration Calorimetry. Experiments were performed on a Microcal ultrasensitive VP-ITC (isothermal titration) calorimeter (MicroCal Inc.). The instrumentation and software for data acquisition/analysis were VPViewer IPC and Microcal Origin (version 5), respectively. Data points were collected every 2 s. Each binding isotherm was determined following 25 automatic injections from an 250 μL injection syringe containing 50 mM Tris-HCl (pH 7.5), 50 mM NaCl, and 1−4 mM $MnCl_2$, into the reaction cell (1.4301 mL) containing 50 mM Tris-HCl (pH 7.5), 50 mM NaCl, and 50−100 μM protein at 30 °C. Injection volumes (5 μL) were delivered over an 10 s time interval with 4 min between injections to allow complete equilibration. Background buffer was the same for both solutions to minimize heat changes from mixing. The data curves were obtained using the resting baseline determined by the software. Data from two or three independent experiments were averaged. Control experiments in the absence of enzyme were used to determine the background heats of dilution.

Determination of Mn^{2+} Content. The wild-type and mutant proteins were dissolved in 50 mM Tris-HCl (pH 7.5) containing 50 mM NaCl and 10 mM $MnCl_2$ and then dialyzed against the same buffer containing 10 μM $MnCl_2$. The number of Mn^{2+} ions remaining bound to the protein after dialysis was determined by atomic absorption spectrometry on a Jarrel-Ash A-8500 Mark II spectrometer.

RESULTS

Mn^{2+}-Dependent Activities of the Active Site Mutants. E. coli RNase HI requires only a few micromolar concentrations of Mn^{2+} for activity at pH 8.0. However, if the binding affinity of the Mn^{2+} ion to the protein were greatly reduced by the mutation, the resultant mutant protein would exhibit the activity only in the presence of higher concentrations of Mn^{2+}. Therefore, the enzymatic activities of the active site mutants D10A, D10N, E48A, E48Q, D70A, D70N, D134A, and D134N were determined at pH 8.0 in the presence of various concentrations of $MnCl_2$ (0.1 μM−10 mM). These activities were not measured at >10 mM $MnCl_2$ because Mn^{2+} is not fully soluble at alkaline pH at such a high concentration. All of these mutant proteins, except for D134N, which is as active as the wild-type protein, do not exhibit the enzymatic activity in the presence of Mg^{2+}. Of these mutant proteins, the D10A, D10N, D70A, and D70N proteins did not exhibit the activity at any condition examined. The other mutant proteins exhibited the Mn^{2+}-dependent activities. However, the dependence of the activity on the Mn^{2+} concentration varied greatly for these proteins (Figure 2A).

The wild-type protein exhibited the maximal specific activity of 15.2 units/mg at 0.5 μM $MnCl_2$ and lower specific activities at >1 μM $MnCl_2$. Its specific activity at 1 mM $MnCl_2$ was 4.2% of the maximal Mn^{2+}-dependent activity, which is 12% of the maximal Mg^{2+}-dependent activity. The D134N protein was also activated at very low Mn^{2+} concentrations but was not inhibited at higher Mn^{2+} concentrations. Consequently, it exhibited the maximal specific

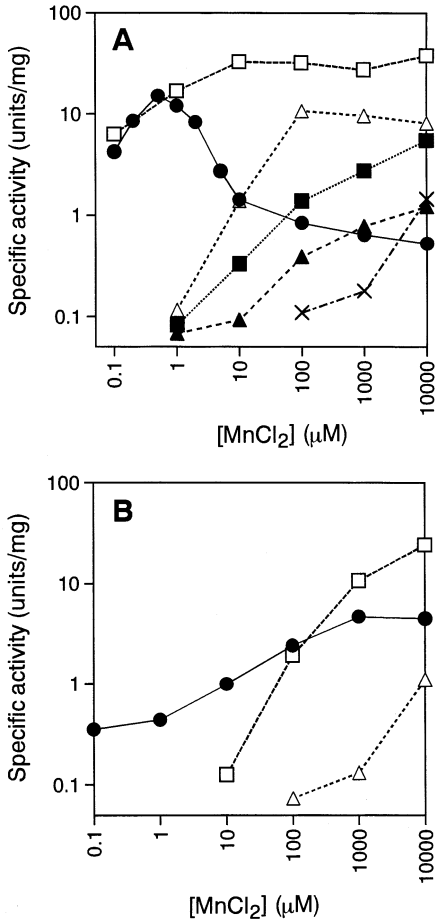

FIGURE 2: Dependence of RNase H activity on Mn^{2+} concentration. The RNase H activity was determined at 30 °C for 15 min in 10 mM Tris-HCl (pH 8.0) (A) or 10 mM MES−NaOH (pH 5.5) (B) containing 50 mM NaCl, 1.4 mM 2-mercaptoethanol, 0.05 mg/mL BSA, and the indicated concentrations (0.1 μM−10 mM) of $MnCl_2$ by using the M13 DNA/RNA hybrid as a substrate. The data for the E48Q, D134A, and E48A/D134N proteins are not shown in Figure 2B, because the activities of these mutant proteins were below the background level at any Mn^{2+} concentration examined. Key: (●) wild type; (△) E48A; (▲) E48Q; (■) D134A; (□) D134N; (×) E48A/D134N.

activity of 33−38 units/mg at >10 μM $MnCl_2$. These results are consistent with those previously reported (*29*, *30*), although the optimum Mn^{2+} concentration for the activity of the wild-type protein is shifted from 2 to 5 μM to 0.5 μM. In contrast, the E48A, E48Q, and D134A proteins required much higher concentrations of Mn^{2+} for activity. As the result, the E48A protein exhibited the maximal specific activity of 10.8 units/mg at 100 μM $MnCl_2$ and was not inhibited at higher Mn^{2+} concentrations. The E48Q and D134A proteins apparently did not exhibit the maximal activity even at 10 mM $MnCl_2$, because their activities kept increasing as the Mn^{2+} concentration increased. The specific activities of the E48Q and D134A proteins at 10 mM $MnCl_2$ were 1.2 and 5.5 units/mg, respectively.

Enzymatic Activities of Double Mutant Proteins. To examine whether the *E. coli* RNase HI variants with double mutations at Glu^{48} and Asp^{134} still exhibit the Mn^{2+}-dependent activities, the E48A/D134A and E48A/D134N proteins were constructed. The cellular production levels of these mutant proteins were lower than that of the wild-type protein by 5−10 times, and the amount of protein purified

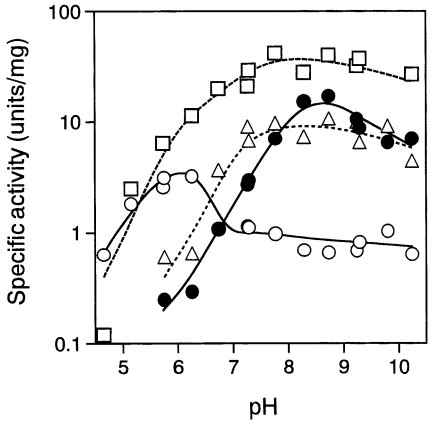

FIGURE 3: pH dependence of Mn^{2+}-dependent activity. The RNase H activity was determined at 30 °C for 15 min at the indicated pH as described in Experimental Procedures by using the M13 DNA/RNA hybrid as a substrate. The activity of the wild-type protein was determined in the presence of either 0.5 μM (●) or 1 mM (○) $MnCl_2$. The activities of the E48A (△) and D134N (□) proteins were determined in the presence of 1 mM $MnCl_2$.

from a 1 L culture was 1−2 mg for these mutant proteins. The far- and near-UV CD spectra of these mutant proteins were nearly identical to those of the wild-type protein (data not shown), suggesting that the protein conformation was not markedly changed by introducing these double mutations. The E48A/D134A protein exhibited little enzymatic activity at any condition examined. In contrast, the E48A/D134N protein exhibited the activity at >1 mM $MnCl_2$ (Figure 2A). Its specific activity at 10 mM $MnCl_2$ was 1.5 units/mg.

Mn^{2+}-Dependent Activity at Acidic pH. The E48A, E48Q, D134A, and E48A/D134N proteins exhibit the RNase H activity only at high Mn^{2+} concentrations, suggesting that the mutations at Glu^{48} or Asp^{134} reduce the binding affinity of Mn^{2+} to the protein. These mutations probably alleviate negative-charge repulsion at the active site and, thereby, either alter the geometry of chelating groups of Mn^{2+} or change the identities of the specific chelating groups at the active site.

At acidic pH, one would expect that the wild-type protein would exhibit activity similar to that of the mutant protein as negative-charge repulsion at the active site is alleviated. Therefore, the enzymatic activities of the wild-type and mutant proteins were analyzed at pH 5.5, an arbitrarily chosen pH in the acidic range, in the presence of various concentrations of $MnCl_2$ (0.1 μM−10 mM). Of them, the wild-type, E48A, and D134N proteins exhibited the activity at any Mn^{2+} concentration examined (Figure 2B). The wild-type protein exhibited the maximal specific activity of 4.7 units/mg at 1 mM $MnCl_2$, which is comparable to that determined at 10 mM $MgCl_2$ (4.9 units/mg), and was not inhibited at higher Mn^{2+} concentrations. The E48A and D134N proteins apparently did not exhibit the maximal activity even at 10 mM $MnCl_2$, because their activities kept increasing as the Mn^{2+} concentration increased. The specific activities of the E48A and D134N proteins at 10 mM $MnCl_2$ were 1.1 and 24.2 units/mg, respectively.

The pH dependence of the activity was also analyzed for the wild-type protein in the presence of either 0.5 μM or 1 mM $MnCl_2$ and the E48A and D134N proteins in the presence of 1 mM $MnCl_2$ (Figure 3). The wild-type protein in the presence of 0.5 μM $MnCl_2$, as well as the mutant

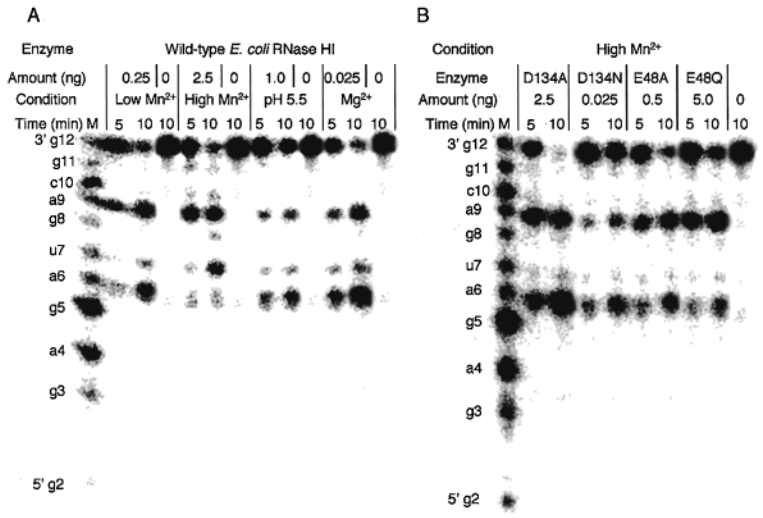

FIGURE 4: Autoradiograph of cleavage reaction products. Hydrolyses of the 5′-labeled 12 bp RNA/DNA hybrid with the wild-type (A) and mutant (B) proteins were carried out at 30 °C for 5 or 10 min at pH 8.0 (10 mM Tris-HCl) or pH 5.5 (10 mM MES−NaOH). The enzyme species, the amount of the enzyme used, and the reaction time are indicated above each lane. Conditions: low Mn^{2+}, 0.5 μM $MnCl_2$ at pH 8.0; high Mn^{2+}, 1.0 mM $MnCl_2$ at pH 8.0; pH 5.5, 1 mM $MnCl_2$ at pH 5.5; Mg^{2+}, 10 mM $MgCl_2$ at pH 8.0. Products were separated on a 20% polyacrylamide gel containing 7 M urea as described in Experimental Procedures. The concentration of the substrate is 1.0 μM. M represents the products generated by partial digestion of the 12 b RNA with snake venom phosphodiesterase. The 3′-terminal residue of each oligonucleotide generated by the partial digestion with snake venom phosphodiesterase is shown along the gel.

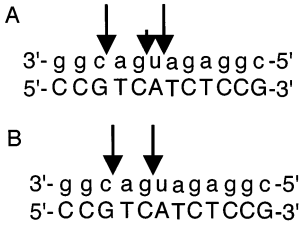

FIGURE 5: Graphical representation of sites and extents of cleavages by RNase H. The cleavage sites of the 12 bp RNA/DNA hybrid with the wild-type protein in the presence of 0.5 μM (A) or 1 mM (B) $MnCl_2$ are shown as representatives. The cleavage sites with the E48A, E48Q, D134A, and D134N proteins are not shown, because they are nearly identical to those with the wild-type protein in the presence of 0.5 μM $MnCl_2$. Differences in the size of the arrows reflect the relative cleavage intensities at the indicated positions. Deoxyribonucleotides are denoted with upper case letters, and ribonucleotides are denoted with lower case letters.

proteins in the presence of 1 mM $MnCl_2$, exhibited the maximal activities at pH 8−9, and their activities greatly decreased as the pH decreased below 7, as did the wild-type protein in the presence of 10 mM $MgCl_2$ (*22*, *35*, *43*). In contrast, the wild-type protein exhibited the maximal activity at pH 6 in the presence of 1 mM $MnCl_2$. These results indicate that high Mn^{2+} concentrations do not significantly contribute to the inhibition of the activity of the wild-type protein at acidic pH.

Cleavage of Oligomeric Substrates in the Presence of Mn^{2+}. To examine whether the cleavage specificity of the enzyme is altered by changing a metal cofactor or by the mutation at Glu^{48} and Asp^{134}, 12 bp RNA/DNA substrate and 29 bp DNA-RNA-DNA/DNA substrate were cleaved by the wild-type and mutant proteins in the presence of Mn^{2+}. The results are shown in Figure 4 and summarized in Figure 5. It has been reported that the wild-type protein hydrolyzes the 12 bp RNA/DNA substrate at multiple sites, but preferentially at a6-u7 and a9-c10, at pH 8.0 in the presence of 10 mM $MgCl_2$ (*44*). The protein cleaved this substrate with a similar sequence specificity either at pH 5.5 in the presence of 1 mM $MnCl_2$ or at pH 8.0 in the presence of 0.5 μM $MnCl_2$. The E48A, E48Q, D134A, and D134N proteins also cleaved it with a similar sequence specificity at pH 8.0 in the presence of 1 mM $MnCl_2$. On the other hand, the wild-type protein cleaved this substrate preferentially at u7-g8 and a9-c10 at pH 8.0 in the presence of 1 mM $MnCl_2$.

The 29 bp DNA−RNA−DNA/DNA substrate has been reported to be cleaved by *E. coli* RNase HI at the middle of the tetraribonucleotide at pH 8.0 in the presence of 10 mM $MgCl_2$ (*2*). All of the wild-type and mutant proteins cleaved this substrate at the same site at any condition examined (data not shown).

Mn^{2+} Binding Monitored by a Change in Protein Stability. To examine whether the elimination of the negative charge at position 10, 48, 70, or 134 affects Mn^{2+} binding, binding of the Mn^{2+} ion to the wild-type and mutant proteins was analyzed by monitoring the changes in the protein stability as described previously for binding of the Mg^{2+} ion (*26*). The $\Delta\Delta G$ value, which is the difference between the ΔG value of the wild-type or the mutant protein in the presence of the Mn^{2+} ion and the ΔG value of the wild-type protein in the absence of the Mn^{2+} ion, is shown as a function of the Mn^{2+} concentration for each protein in Figure 6. From these data, two different dissociation constants, K_{d1} and K_{d2}, were calculated on the assumption that two Mn^{2+} ions bind to the wild-type protein in its native state. Likewise, the dissociation constant K_d was calculated on the assumption that one Mn^{2+} ion binds to the mutant proteins. These values are summarized in Table 1. The K_d value for binding of the Mn^{2+} ion to the wild-type protein was also calculated to be 5.48 μM on the assumption that one Mn^{2+} ion binds to the protein. This value is similar to the K_{d1} value (5.08 μM), suggesting that binding of the first Mn^{2+} ion mainly contributes to the increase in the protein stability upon Mn^{2+} binding. For each protein, the plots of $\Delta\Delta G$ versus the concentration of the Mn^{2+} ion, in which the $\Delta\Delta G$ values were calculated by using these K_d values (for mutant proteins) or K_{d1} and K_{d2}, values (for wild type), fit well with the

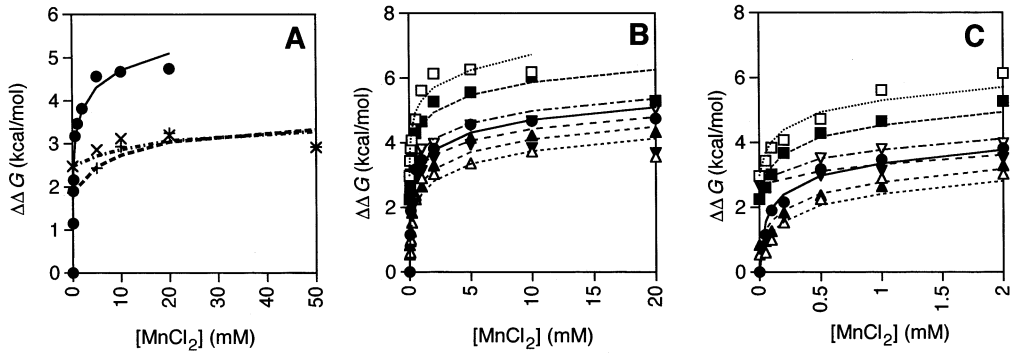

FIGURE 6: Plot of $\Delta\Delta G$ as a function of the concentration of added $MnCl_2$. The $\Delta\Delta G$ values were calculated from the ΔT_m values as previously described (*26*). Symbols indicate the experimental data: (●) wild type; (×) D10N; (△) E48A; (▲) E48Q; (+) D70N; (□) D134A; (■) D134N; (▽) E48A/D134A; (▼) E48A/D134N. The lines represent the best fit to the experimental data calculated by using Mn^{2+} dissociation constants of these proteins according to the equation given in Experimental Procedures. The $\Delta\Delta G$ value is the difference between the ΔG value of the wild-type or mutant protein in the presence of the Mn^{2+} ion and the ΔG value of the wild-type protein in the absence of the Mn^{2+} ion. The data are commonly expressed in panels A−C, which differ from one another only in the abscissa scale ($MnCl_2$ concentration). The plots for E48Q, E48A, D134N, D134A, E48A/D134N, and E48A/D134A are removed from panel A, and the plots of D10N and D70N are removed from panels B and C, for clarification.

Table 1: Dissociation Constants of Mn^{2+}

protein	K_d (μM) stability[a]	K_d (μM) calorimetry[b]
WT	5.08 (K_{d1})	4.32
	1100 (K_{d2})	ND[c]
D10N	8820	ND
D10A	ND	no binding
E48A	52.3	9.14
E48Q	46.5	ND
D70N	2250	ND
D134A	25.2	ND
D134N	27.3	ND
E48A/D134N	1310	ND
E48A/D134A	330	131

[a] The binding of Mn^{2+} to the protein was analyzed by monitoring a change in the protein stability upon Mn^{2+} binding, as described in Experimental Procedures. The dissociation constants of the Mn^{2+} ion were calculated on an assumption that two Mn^{2+} ions bind to the wild-type protein with the dissociation constants of K_{d1} and K_{d2} or one Mn^{2+} ion binds to the mutant proteins with the dissociation constant of K_d. Errors are within 10% of the values reported. [b] The binding of Mn^{2+} to the protein was analyzed by direct calorimetry as described in Experimental Procedures. Errors are within 12% of the values reported. [c] ND: not determined.

experimental data (Figure 6). The dissociation constants for the binding of the Mn^{2+} ion to the D10N and D70N proteins were increased by 1.7×10^3- and 4.4×10^2-fold, respectively, as compared to that (K_{d1}) of the wild-type protein. These results suggest that the binding affinity of the Mn^{2+} ion to the protein is greatly reduced by the elimination of the negative charge at either position 10 or position 70. The dissociation constants for the binding of Mn^{2+} ion to the E48A, E48Q, D134A, D134N, E48A/D134A, and E48A/D134N proteins are increased by 10-, 9.2-, 5.0-, 5.4-, 65-, and 260-fold, respectively, as compared to that (K_{d1}) of the wild-type protein. These results suggest that the binding affinity of the Mn^{2+} ion to the protein is also reduced by the elimination of the negative charge at either position 48 or position 134, but to a lesser extent.

The number of the Mn^{2+} ions which remained bound to the protein after dialysis was determined by atomic absorption spectrometry to be 0.93 ± 0.05 for wild type, 0.07 ± 0.03 for D10A, 0.94 ± 0.05 for E48A, and 0.23 ± 0.04 for E48A/D134A.

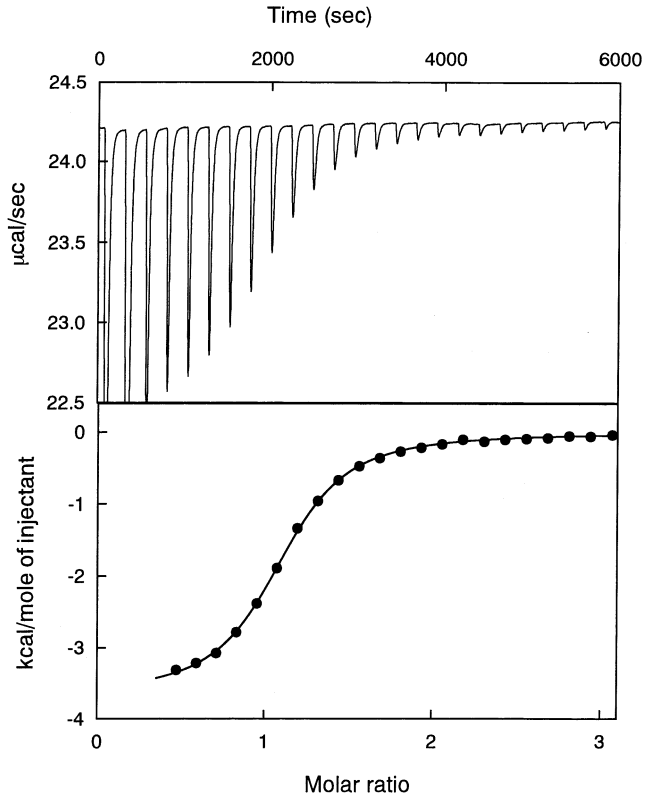

FIGURE 7: Titration of *E. coli* RNase HI with Mn^{2+}. The titration calorimetry was carried out at pH 7.5 and 30 °C as described in Experimental Procedures. The raw data are shown in upper panel and the integrated data in the lower panel. The line in the lower panel represents the optimal fit to the data.

Calorimetric Titration with Mn^{2+}. Binding of the Mn^{2+} ion to the wild-type, D10A, E48A, and E48A/D134A proteins was also analyzed by direct titration calorimetry. Heat changes upon Mn^{2+} binding were not observed for D10A but observed for other proteins, indicating that the Mn^{2+} ion does not bind or poorly binds to the D10A protein. The results obtained for the wild-type protein are shown in Figure 7, as a representative. From these results, the number of the Mn^{2+} ion bound to the protein was calculated to be 1.07 ± 0.04 for wild-type, 0.90 ± 0.04 for E48A, and 0.59 ± 0.15 for E48A/D134A proteins. The dissociation

constant of the Mn^{2+} ion for binding to the wild-type protein (4.32 μM), which may represent that of the first Mn^{2+} ion, was comparable to that determined by monitoring a change in protein stability upon Mn^{2+} binding. As compared to this value, the K_d values for binding of the Mn^{2+} ion to the E48A and E48A/D134A proteins were increased by 2.1- and 30-fold, respectively (Table 1). The dissociation constant of the second Mn^{2+} ion could not be determined, because the protein was precipitated upon titration with Mn^{2+} when the concentrations of the protein and $MnCl_2$ were increased by 10 times. It is necessary to increase these concentrations by at least 10 times to detect a weak interaction between the second Mn^{2+} ion and the protein.

DISCUSSION

Physiological Role of the Second Metal-Binding Site. The physiological significance of the second metal-binding site (site 2) remains to be determined. However, the E48A and D134A proteins did not complement the temperature-sensitive growth phenotype of the *rnhA* mutant strain *E. coli* MIC3001 (*45*) (data not shown). These mutant proteins exhibit the RNase H activity at high Mn^{2+} concentrations, at which the activity of the wild-type protein is attenuated upon binding of the second Mn^{2+} ion. Therefore, the concentration of the Mn^{2+} ion in the bacterial cells may be too low to activate these mutant proteins and convert the wild-type protein to the two-metal form.

Possible Catalytic Mechanism of RNase HI in the Two-Mn^{2+} Form. E. coli RNase HI contains two metal-binding sites (Figure 1). It has been proposed that one Mn^{2+} ion binds to the "activation" site (site 1) at low Mn^{2+} concentrations (<1 μM) and the second Mn^{2+} ion binds to the "attenuation" site (site 2) at high Mn^{2+} concentrations (>10 μM), whereas only one Mg^{2+} ion binds to site 1, even at high Mg^{2+} concentrations (>0.5 mM) (*24*, *30*). However, the protein is not fully inactivated upon binding of the second Mn^{2+} ion, as indicated by the fact that it retained 3.5% of the maximal activity even at 10 mM $MnCl_2$. In addition, the cleavage specificity of the protein determined at pH 8.0 and 1 mM $MnCl_2$ was slightly, but significantly, different from that determined at pH 8.0 and 0.5 μM $MnCl_2$ or 10 mM $MgCl_2$ (Figures 4 and 5). In addition, both k_{cat} and K_m values of the protein determined in the presence of high concentrations of Mn^{2+} were reduced significantly as compared to those determined in the presence of low concentrations of Mn^{2+} (*30*). These results strongly suggest that, in terms of its catalytic mechanism, the protein in the two-Mn^{2+} form exhibits activity distinguishable from that of the protein in the one-Mn^{2+} form.

A possible catalytic mechanism for the activity of the protein in two-Mn^{2+} form is shown in Figure 8B. According to this mechanism, the second Mn^{2+} ion, instead of His^{124}, facilitates the formation of an attacking hydroxide ion, as reported for the 3′ to 5′ exonuclease (*46*). His^{124} has been proposed to act as a proton pump and activate an attacking H_2O molecule (general base) when Mg^{2+} is used as a metal cofactor (Figure 8A) (*20*). However, this function of His^{124} may be inhibited upon binding of the second Mn^{2+} ion at site 2, because His^{124} is located in the vicinity of this site. In fact, the His^{124} → Ala mutation greatly reduces the activities of the protein at high Mg^{2+} (*32*) and low Mn^{2+} (*30*) concentrations but does not seriously affect it at high Mn^{2+} concentrations (*30*).

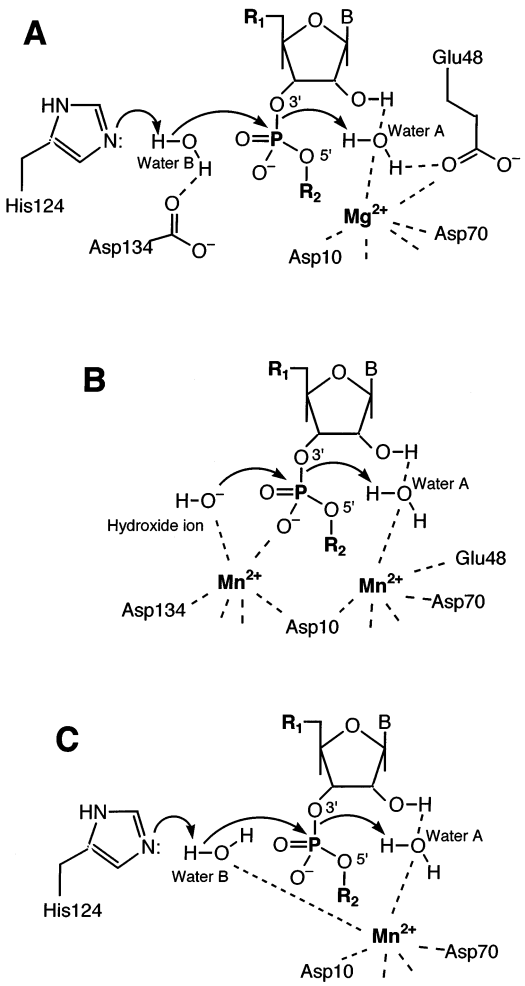

FIGURE 8: Proposed catalytic mechanisms of *E. coli* RNase HI. Possible catalytic mechanisms of *E. coli* RNase HI in one-Mg^{2+} (A), two-Mn^{2+} (B), and one-Mn^{2+} (C) forms are represented schematically. Water A and Water B represent the water molecules that act as a general acid and a general base, respectively. A catalytic mechanism of the protein in one-Mg^{2+} form (A) has previously been proposed (*26*). In a catalytic mechanism of the protein in two-Mn^{2+} form (B), all four conserved acidic residues, Asp^{10}, Glu^{48}, Asp^{70}, and Asp^{134}, are required for coordination with two Mn^{2+} ions. His^{124} is not shown because it may not be involved in catalysis. The second Mn^{2+} ion which coordinates with Asp^{10} and Asp^{134}, instead of His^{124}, facilitates the formation of an attacking hydroxide ion. In a catalytic mechanism of the protein in one-Mn^{2+} form (C), Asp^{10} and Asp^{70} are required for coordination with one Mn^{2+} ion. Glu^{48} and Asp^{134} are not shown because they are dispensable for activity. His^{124} activates the water B molecule as a proton pump.

Atomic absorption spectrometry and direct titration calorimetry indicated that one Mn^{2+} ion tightly binds to the protein. The binding of the second Mn^{2+} ion to the protein was not detected by these analyses, probably because the binding affinity of the second Mn^{2+} ion is much lower than that of the first Mn^{2+} ion. The dissociation constant of the first Mn^{2+} ion was determined to be 4.32 μM by direct titration calorimetry and 5.08 μM by thermal denaturation experiments. The dissociation constant of the Mg^{2+} ion has previously been determined to be 200 μM (*27*) or 710 μM (*26*). Therefore, the binding affinity of the first Mn^{2+} ion was shown to be higher than that of the Mg^{2+} ion by ~100 fold. This difference in binding affinity may account for the

difference in the maximal number of the Mn^{2+} and Mg^{2+} ions bound to the protein.

Possible Catalytic Mechanism of RNase HI in the One-Mn^{2+} Form. It has previously been reported that the *E. coli* RNase HI variant, which lacks the C-terminal helix containing Asp^{134} (*47*), and the HIV-1 RT variant, in which Glu^{478} (corresponding to Glu^{48} of *E. coli* RNase HI) is replaced by Gln (*48*), do not exhibit the Mg^{2+}-dependent activity but exhibit the Mn^{2+}-dependent activity. These findings support our conclusion in this report that Glu^{48} and Asp^{134} are dispensable for Mn^{2+}-dependent activity of *E. coli* RNase HI. Furthermore, these results, as well as those obtained from the binding analyses of the Mn^{2+} ion, indicate that the carboxyl groups of Asp^{10} and Asp^{70} are responsible for Mn^{2+} binding. The importance of two carboxylates, which are corresponding to Asp^{10} and Asp^{70} of *E. coli* RNase HI, for Mn^{2+} binding have also been reported for HIV-1 RT (*49*) and the RNase H domain of Moloney murine leukemia virus RT (*50*). It has been reported that the latter protein has a strong preference for Mn^{2+} (*51*). Therefore, it would be informative to examine whether all four conserved acidic residues in this protein are required for activity.

The E48A, E48Q, and D134A proteins exhibited the Mn^{2+}-dependent activities only at high Mn^{2+} concentrations (Figure 2A). Atomic absorption spectrometry and direct titration calorimetry indicated that one Mn^{2+} ion binds to the E48A and E48A/D134A proteins. Determination of the dissociation constant of the Mn^{2+} ion by direct titration calorimetry and thermal denaturation experiments indicated that the binding affinity of the Mn^{2+} ion to the protein is reduced by 2−10 times by the mutation at Glu^{48} or Asp^{134}. Therefore, the mutations at Glu^{48} and Asp^{134} equally reduce the binding affinity of the Mn^{2+} ion, probably because they alter the geometry of chelating groups of Mn^{2+} or change chelating groups at the active site, and thereby only permit binding of one Mn^{2+} ion to the protein, even at high Mn^{2+} concentrations. It is unlikely that these activities represent that of the enzyme in the two-Mn^{2+} form, because the cleavage specificities of these mutant proteins are nearly identical to that of the enzyme in the one-metal form (Figures 4 and 5), and the maximal specific activities of the E48A and D134A proteins are comparable to that of the wild-type protein (Mn^{2+}-dependent activity) (Figure 2A).

Because Glu^{48} and Asp^{134} are constituents of site 1 and site 2, respectively (Figure 1), the question arises whether the E48A and D134A proteins are activated upon binding of one Mn^{2+} ion at site 1 or site 2. To answer this question, it will be necessary to determine the crystal structure of these mutant proteins in complex with Mn^{2+}. However, the E48A and D134A proteins are not distinguishable from each other, in terms of maximal specific activity (Figure 2A) and cleavage specificity of the substrate (Figures 4 and 5), suggesting that both mutant proteins share a common Mn^{2+} binding site. If the Mn^{2+}-binding site were shifted by 4 Å, which is the distance between site 1 and site 2, the cleavage specificity and/or the specific activity of the enzyme would be significantly altered. Therefore, it seems likely that the E48A, E48Q, and D134A proteins are activated upon binding of one Mn^{2+} ion at site 1 or a nearby site. According to the crystallographic studies (*23*, *24*), Glu^{48} provides a ligand for both Mg^{2+} and Mn^{2+} bindings at site 1. However, Mg^{2+} titration experiments monitored by a change in protein stability have suggested that the carboxyl group of Glu^{48} is not responsible for Mg^{2+} binding (*26*).

A possible catalytic mechanism for the activity of the protein in the one-Mn^{2+} form is shown in Figure 8C. The protein is activated upon binding of one Mn^{2+} or Mg^{2+} ion at site 1 or a nearby site. However, the catalytic mechanisms of the enzyme upon binding of each ion may be different from each other, because Glu^{48} and Asp^{134} are dispensable for Mn^{2+}-dependent activity. It has been proposed that Glu^{48} (*26*) and Asp^{134} (*35*) are required to hold H_2O molecules that act as a general acid and general base, respectively (Figure 8A). However, these residues are required to hold H_2O molecules only when Mg^{2+} is used as a metal cofactor. When Mn^{2+} is used as a metal cofactor, the Mn^{2+} ion itself may hold these H_2O molecules (Figure 8C). The role of the metal ion in catalytic function varies for Mg^{2+} and Mn^{2+}, probably because Mn^{2+} is a transition metal and coordinates with a different geometry than Mg^{2+}.

Binding of Mn^{2+} Ion at Acidic pH. The wild-type, E48A, and D134N proteins exhibited the Mn^{2+}-dependent activities at pH 5.5 as well but only at high Mn^{2+} concentrations (Figure 2B). Because the cleavage specificity of the wild-type protein at pH 5.5 and 1 mM $MnCl_2$ is nearly identical to that at pH 8.0 and 0.5 μM $MnCl_2$ (Figures 4 and 5), and its maximal specific activity at pH 5.5 is 30% of the maximal Mn^{2+}-dependent activity at pH 8.0, these activities may represent those of the proteins in the one-Mn^{2+} form. The Mn^{2+} ion probably binds to site 1 or a nearby site with much weaker affinity at pH 5.5. At acidic pH, one or more carboxylates at the active site may be protonated such that the geometry of the chelating groups of Mn^{2+} becomes similar to that of the mutant protein at alkaline pH. Indeed, the wild-type protein exhibited activity at pH 5.5 similar to that of the mutant protein at pH 8.0. Alternatively, the specific chelating groups at the active site are changed, another possible scenario that may explain the lower binding affinity of the mutant proteins for Mn^{2+}.

Validity of Catalytic Mechanisms. The catalytic mechanisms mentioned above may be valid, because they are proposed not only on the basis of structural and biophysical studies of the proteins in the absence of the substrate but also on detailed studies of the enzymatic properties of a variety of the active site mutants. However, the protein exhibited maximal Mn^{2+}-dependent activity at lower Mn^{2+} concentrations than that predicted from the dissociation constant of Mn^{2+} determined in the absence of the substrate (Figure 2A). It has also been reported that both the k_{cat} and K_m values of the protein are reduced significantly upon binding of the second Mn^{2+} ion (*30*). These results suggest that binding affinity of the Mn^{2+} ion is increased in the presence of the substrate, probably because the negative-charge density at the active site is increased upon binding of the substrate and, reciprocally, that the Mn^{2+} ion strengthens the interaction between the protein and substrate. Therefore, the binding sites and dissociation constants of the metal ions and the number of the metal ions bound to the protein may be altered in the absence of the substrate. To understand a role of the metal cofactor in catalytic function, it will be necessary to determine the crystal structure of the protein in complex with a substrate and a metal cofactor.

The crystal structure of HIV-1 RT in complex with an RNA/DNA hybrid containing a polypurine tract (PPT) has

recently been determined (*52*). This structure is consistent with a model for the complex between *E. coli* RNase HI and the RNA/DNA hybrid (*53*). According to this structure, a structural element termed "RNase H primer grip" determines the trajectory of the RNA strand in relation to the RNase H active site by interacting with the DNA strand. The RNA strand can contact with the active site only when an RNA/DNA substrate has an appropriate minor groove width. Because PPT has an unusually narrow minor groove, the RNA strand is located too far from the active site (~3 Å away) to be hydrolyzed, although His^{539}, which is corresponding to His^{124} of *E. coli* RNase HI, contacts the RNA strand at a scissible phosphate group.

REFERENCES

1. Crouch, R. J., and Dirksen, M.-L. (1982) in *Nuclease* (Linn, S. M., and Roberts, R. J., Eds.) pp 211−241, Cold Spring Harbor Laboratory, Cold Spring Harbor, NY.
2. Ohtani, N., Haruki, M., Morikawa, M., Crouch, R. J., Itaya, M., and Kanaya, S. (1999) *Biochemistry 38*, 605−618.
3. Ohtani, N., Haruki, M., Morikawa, M., and Kanaya, S. (1999) *J. Biosci. Bioeng. 88*, 12−19.
4. Itaya, M., Omori, A., Kanaya, S., Crouch, R. J., Tanaka, T., and Kondo, K. (1999) *J. Bacteriol. 181*, 2118−2123.
5. Arudchandran, A., Cerritelli, S., Narimatsu, S., Itaya, M., Shin, D. Y., Shimada, Y., and Crouch, R. J. (2000) *Genes Cells 5*, 789−802.
6. Kanaya, S., and Ikehara, M. (1995) in *Subcellular Biochemistry, Vol. 24. Proteins: Structure, Function, and Engineering* (Biswas, B. B., and Roy, S., Eds.) pp 377−422, Plenum Press, New York.
7. Kogoma, T., and Foster, P. L. (1998) in *Ribonucleases H* (Crouch, R. J., and Toulme, J. J., Eds.) pp 39−66, INSERM, Paris.
8. Murante, R. S., Henricksen, L. A., and Bambara R. A. (1998) *Proc. Natl. Acad. Sci. U.S.A. 95*, 2244−2249.
9. Qiu, J., Qian, Y., Frank, P., Wintersberger, U., and Shen, B. (1999) *Mol. Cell. Biol. 19*, 8361−8371.
10. Hughes, S. H., Arnold, E., and Hostomsky, Z. (1998) in *Ribonucleases H* (Crouch, R. J., and Toulme, J. J., Eds.) pp 195−224, INSERM, Paris.
11. Yang, W., Hendrickson, W. A., Crouch, R. J., and Satow, Y. (1990) *Science 249*, 1398−1405.
12. Katayanagi, K., Miyagawa, M., Matsushima, M., Ishikawa, M., Kanaya, S., Ikehara, M., Matsuzaki, T., and Morikawa, K. (1990) *Nature 347*, 306−309.
13. Muroya, A., Tsuchiya, D., Ishikawa, M., Haruki, M., Morikawa, M., Kanaya, S., and Morikawa, K. (2001) *Protein Sci. 10*, 707−714.
14. Ariyoshi, M., Vassylyev, D. G., Iwasaki, H., Nakamura, H., Shinagawa, H., and Morikawa, K. (1994) *Cell 78*, 1063−1072.
15. Dyda, F., Hickman, A. B., Jenkins, T. M., Engelman, A., Craigie, R., and Davies, D. R. (1994) *Science 266*, 1981−1986.
16. Buiacz, G., Jaskolski, M., Alexandratos, J., Wlodawer, A., Merkel, G., Katz, R. A., and Skalka, A. M. (1996) *Structure 4*, 89−96.
17. Rice, P., and Mizuuchi, K. (1995) *Cell 82*, 209−220.
18. Mol, C. D., Kuo, C. F., Thayer, M. M., Cunningham, R. P., and Trainer, J. A. (1995) *Nature 374*, 381−386.
19. Blaszczyk, J., Tropea, J. E., Bubunenko, M., Routzahn, K. M., Waugh, D. S., Court, D. L., and Ji, X. (2001) *Structure 9*, 1225−1236.
20. Kanaya, S. (1998) in *Ribonucleases H* (Crouch, R. J., and Toulme, J. J., Eds.) pp 1−38, INSERM, Paris.
21. Kanaya, S., and Crouch, R. J. (1983) *J. Biol. Chem. 258*, 1276−1281.
22. Berkower, I., Leis, J., and Hurwitz, J. (1973) *J. Biol. Chem. 248*, 5914−5921.
23. Katayanagi, K., Okumura, M., and Morikawa, K. (1993) *Proteins: Struct., Funct., Genet. 17*, 337−346.
24. Goedken, E. R., and Marqusee, S. (2001) *J. Biol. Chem. 276*, 7266−7271.
25. Oda, Y., Nakamura, H., Kanaya, S., and Ikehara, M. (1991) *J. Biomol. NMR 1*, 247−255.
26. Kanaya, S., Oobatake, M., and Liu, Y. Y. (1996) *J. Biol. Chem. 271*, 32729−32736.
27. Huang, H. W., and Cowan, J. A. (1994) *Eur. J. Biochem. 219*, 253−260.
28. Davies, J. F., Hostomska, Z., Hostomsky, Z., Jordan, S. R., and Matthews, D. A. (1991) *Science 252*, 88−95.
29. Keck, J. L., and Marqusee, S. (1996) *J. Biol. Chem. 271*, 19883−19887.
30. Keck, J. L., Goedken, E. R., and Marqusee, S. (1998) *J. Biol. Chem. 273*, 34128−34133.
31. Kanaya, S., Kohara, A., Miura, Y., Sekiguchi, A., Iwai, S., Inoue, H., Ohtsuka, E., and Ikehara, M. (1990) *J. Biol. Chem. 265*, 4615−4621.
32. Oda, Y., Yoshida, M., and Kanaya, S. (1993) *J. Biol. Chem. 268*, 88−92.
33. Haruki, M., Noguchi, E., Nakai, C., Liu, Y. Y., Oobatake, M., Itaya, M., and Kanaya, S. (1994) *Eur. J. Biochem. 220*, 623−631.
34. Katayanagi, K., Ishikawa, M., Okumura, M., Ariyoshi, M., Kanaya, S., Kawano, Y., Suzuki, M., Tanaka, I., and Morikawa, K. (1993) *J. Biol. Chem. 268*, 22092−22099.
35. Kashiwagi, T., Jeanteur, D., Haruki, M., Katayanagi, K., Kanaya, S., and Morikawa, K. (1996) *Protein Eng. 9*, 857−867.
36. Kanaya, S., Oobatake, M., Nakamura, H., and Ikehara, M. (1993) *J. Biotechnol. 28*, 117−136.
37. Kanaya, S., Kimura, S., Katsuda, C., and Ikehara, M. (1990) *Biochem. J. 271*, 59−66.
38. Laemmli, U. K. (1970) *Nature 227*, 680−685.
39. Kanaya, S., Katsuda, C., Kimura, S., Nakai, T., Kitakuni, E., Nakamura, H., Katayanagi, K., Morikawa, K., and Ikehara, M. (1991) *J. Biol. Chem. 266*, 6038−6044.
40. Jay, E., Bambara, R., Padmanabham, P., and Wu, R. (1974) *Nucleic Acids Res. 1*, 331−353.
41. Kimura, S., Nakamura, H., Hashimoto, T., Oobatake, M., and Kanaya, S. (1992) *J. Biol. Chem. 267*, 21535−21542.
42. Schellman, J. A. (1975) *Biopolymers 14*, 999−1018.
43. Casareno, R. L. B., Li, D., and Cowan, J. A. (1995) *J. Am. Chem. Soc. 117*, 11011−11012.
44. Kanaya, E., and Kanaya, S. (1995) *Eur. J. Biochem. 231*, 557−562.
45. Itaya, M., and Crouch, R. J. (1991) *Mol. Gen. Genet. 227*, 424−432.
46. Beese, L. S., and Steitz, T. A. (1991) *EMBO J. 10*, 25−33.
47. Goedken, E. R., Raschke, T. M., and Marqusee, S. (1997) *Biochemistry 36*, 7256−7263.
48. Cirino, N. M., Cameron, C. E., Smith, J. S., Rausch, J. W., Roth, M. J., Benkovic, S. J., and Le Grice, S. F. J. (1995) *Biochemistry 34*, 9936−9943.
49. Cowan, J. A., Ohyama, T., Howard, K., Rausch, J. W., Cowan, S. M. L., and Le Grice, S. F. J. (2000) *J. Biol. Inorg. Chem. 5*, 67−74.
50. Goedken, E. R., and Marqusee, S. (1999) *Protein Eng. 12*, 975−980.
51. Zhan, X., and Crouch, R. J. (1997) *J. Biol. Chem. 272*, 22023−22029.
52. Sarafianos, S. G., Das, K., Tantillo, C., Clark, A. D., Jr., Ding, J., Whitcomb, J. M., Boyer, P. L., Hughes, S. H., and Arnold, E. (2001) *EMBO J. 20*, 1449−1461.
53. Nakamura, H., Oda, Y., Iwai, S., Inoue, H., Ohtsuka, E., Kanaya, S., Kimura, S., Katsuda, C., Katayanagi, K., Morikawa, K., Miyashiro, H., and Ikehara, M. (1991) *Proc. Natl. Acad. Sci. U.S.A. 88*, 11535−11539.

BI0205606